

# Modal expansions and non-perturbative quantum field theory in Minkowski space

Nathan Salwen\*  
*Harvard University*  
*Cambridge, MA 02138*

Dean Lee†  
*University of Massachusetts*  
*Amherst, MA 01003*

September 1, 2018

## Abstract

We introduce a spectral approach to non-perturbative field theory within the periodic field formalism. As an example we calculate the real and imaginary parts of the propagator in  $1 + 1$  dimensional  $\phi^4$  theory, identifying both one-particle and multi-particle contributions. We discuss the computational limits of existing diagonalization algorithms and suggest new quasi-sparse eigenvector methods to handle very large Fock spaces and higher dimensional field theories. [PACS numbers: 11.10Kk, 12.38Lg]

## 1 Introduction

Modal expansion methods have recently been used to study non-perturbative phenomena in quantum field theory [1]-[3]. Modal field theory, the name for the general procedure, consists of two main parts. The first is to approximate field theory as a finite-dimensional quantum mechanical system. The second is to analyze the properties of the reduced system using one of several computational techniques. The quantum mechanical approximation is generated by decomposing field configurations into free wave modes. This technique has been explored using both spherical partial waves (spherical field theory [1][2]) and periodic box modes (periodic field theory [3]).

Having reduced field theory to a more tractable quantum mechanical system, we have several different ways to proceed. Boson interactions in Euclidean space, for example, can be modeled using the method of diffusion Monte Carlo. In many situations, however, Monte Carlo techniques are inadequate. These include unquenched fermion systems, processes in Minkowski space, and the phenomenology of multi-particle states. Difficulties arise when the functional

---

\*email: salwen@physics.harvard.edu

†email: dlee@physics.umass.edu

integral measure cannot be treated as a probability distribution or when information must be extracted from excited states obscured by dominant lower lying states. Fortunately there are several alternative methods in the modal field formalism which avoid these problems. Matrix Runge-Kutta techniques were introduced in [2] as a method for calculating unquenched fermion interactions. Here we discuss a different approach, one which directly calculates the spectrum and eigenstates of the Hamiltonian. For this approach it is essential that the Hamiltonian is time-independent, and so we will consider periodic rather than spherical field theory. As we demonstrate, these methods naturally accommodate the study of multi-particle states and Minkowskian dynamics.

We apply the spectral approach to  $1 + 1$  dimensional  $\phi^4$  theory in a periodic box and calculate the real and imaginary parts of the  $\phi$  propagator. Some interesting properties of  $\phi_2^4$  theory such as the phase transition at large coupling were already discussed within the modal field formalism using Euclidean Monte Carlo techniques [3]. The purpose of this analysis is of a more general and exploratory nature. Our aim is to test the viability of modal diagonalization techniques for quantum field Hamiltonians. We would like to know whether we can clearly see multi-particle phenomena, the size of the errors and computational limitations with current computer resources, and how such methods might be extended to more complicated higher dimensional field theories.

The spectral method presented in the first part of our analysis is similar to the work of Brooks and Frautschi [4],<sup>1</sup> who considered a  $1 + 1$  dimensional Yukawa model in a periodic box and deserves credit for the first application of diagonalization techniques using plane wave modes in a periodic box. Our calculations are also similar in spirit to diagonalization-based Hamiltonian lattice formulations [5] and Tamm-Dancoff light-cone and discrete light-cone quantization [6]-[8]. There are, however, some differences which we should mention. As in [4] we are using a momentum lattice rather than a spatial lattice. We find this convenient to separate out invariant subspaces according to total momentum quantum numbers. Since we are using an equal time formulation our eigenvectors are not boost invariant as they would be on the light cone. Also we are using a simple momentum cutoff scheme rather than a regularization scheme which includes Tamm-Dancoff Fock-space truncation. As a result our renormalization procedure is relatively straightforward, but we will have to confront the problem of diagonalizing large Fock spaces from the very beginning. In the latter part of the paper we mention current work on quasi-sparse eigenvector methods which can handle even exceptionally large Fock spaces. Despite the differences among the various diagonalization approaches to field theory, the issues and problems discussed in our analysis are of a general nature. We hope that the ideas presented here will be of use for the various different approaches.

---

<sup>1</sup>We thank the referee of the original manuscript for providing information on this reference.

## 2 Spectral method

The field configuration  $\phi$  in 1 + 1 dimensions is subject to periodic boundary conditions  $\phi(t, x - L) = \phi(t, x + L)$ . Expanding in terms of periodic box modes, we have

$$\phi(t, x) = \sqrt{\frac{1}{2L}} \sum_{n=0, \pm 1, \dots} \phi_n(t) e^{in\pi x/L}. \quad (1)$$

The sum over momentum modes is regulated by choosing some large positive number  $N_{\max}$  and throwing out all high-momentum modes  $\phi_n$  such that  $|n| > N_{\max}$ . In this theory renormalization can be implemented by normal ordering the  $\phi^4$  interaction term. After a straightforward calculation (details are given in [3]), we find that the counterterm Hamiltonian has the form

$$\frac{6\lambda b}{4!2L} \sum_{n=-N_{\max}, N_{\max}} \phi_{-n} \phi_n, \quad (2)$$

where

$$b = \sum_{n=-N_{\max}, N_{\max}} \frac{1}{2\omega_n}, \quad \omega_n = \sqrt{\frac{n^2 \pi^2}{L^2} + \mu^2}. \quad (3)$$

We represent the canonical conjugate pair  $\phi_n$  and  $\frac{d\phi_{-n}}{dt}$  using the Schrödinger operators  $q_n$  and  $-i\frac{\partial}{\partial q_n}$ . Then the functional integral for  $\phi^4$  theory is equivalent to that for a quantum mechanical system with Hamiltonian

$$H = \sum_{n=-N_{\max}, N_{\max}} \left[ -\frac{1}{2} \frac{\partial}{\partial q_{-n}} \frac{\partial}{\partial q_n} + \frac{1}{2} (\omega_n^2 - \frac{\lambda b}{4L}) q_{-n} q_n \right] \quad (4)$$

$$+ \frac{\lambda}{4!2L} \sum_{\substack{n_i=-N_{\max}, N_{\max} \\ n_1+n_2+n_3+n_4=0}} q_{n_1} q_{n_2} q_{n_3} q_{n_4}.$$

We now consider the Hilbert space of our quantum mechanical system. Given  $d$ , an array of non-negative integers,

$$d = \{d_{-N_{\max}}, \dots, d_{N_{\max}}\}, \quad (5)$$

we denote  $p_d(q)$  as the following monomial with total degree  $|d|$ ,

$$p_d(q) = \prod_{n=-N_{\max}, N_{\max}} q_n^{d_n}, \quad \sum_n d_n = |d|. \quad (6)$$

We define  $G_\zeta(q)$  to be a Gaussian of the form<sup>2</sup>

$$G_\zeta(q) = \prod_{n=-N_{\max}, N_{\max}} \exp \left[ -\frac{q_{-n} q_n \sqrt{\zeta^2 + n^2 \pi^2 / L^2}}{2} \right]. \quad (7)$$

---

<sup>2</sup> $G_\zeta(q)$  has been defined such that  $G_\mu(q)$  is the ground state of the free theory.

$\zeta$  is an adjustable parameter which we will set later. Any square-integrable function  $\psi(q)$  can be written as a superposition

$$\psi(q) = \sum_d c_d p_d(q) G_\zeta(q). \quad (8)$$

In this analysis we consider only the zero-momentum subspace. We impose this constraint by restricting the sum in (8) to monomials satisfying

$$\sum_n n d_n = 0. \quad (9)$$

We will restrict the space of functions  $\psi(q)$  further by removing high energy states in the following manner. Let

$$k(d) = \sum_n |n| d_n. \quad (10)$$

$k(d)$  was first introduced in [2] and provides an estimate of the kinetic energy associated with a given state. Let us define two auxiliary cutoff parameters,  $K_{\max}$  and  $D_{\max}$ . We restrict the sum in (8) to monomials such that  $k(d) < K_{\max}$  and  $|d| \leq D_{\max}$ . We will refer to the corresponding subspace as  $V_{K_{\max}, D_{\max}}$ . The cutoff  $K_{\max}$  removes states with high kinetic energy and the cutoff  $D_{\max}$  eliminates states with a large number of excited modes.<sup>3</sup> We should stress that  $K_{\max}$  and  $D_{\max}$  are only auxiliary cutoffs. We increase these parameters until the physical results appear close to the asymptotic limit  $K_{\max}, D_{\max} \rightarrow \infty$ . In our scheme ultraviolet regularization is provided only by the momentum cutoff parameter  $N_{\max}$ .

Our plan is to analyze the spectrum and eigenstates of  $H$  restricted to this approximate low energy subspace,  $V_{K_{\max}, D_{\max}}$ . For any fixed  $L$  and  $N_{\max}$ ,  $H$  is the Hamiltonian for a finite-dimensional quantum mechanical system and the results should converge in the limit  $K_{\max}, D_{\max} \rightarrow \infty$ . We obtain the desired field theory result by then taking the limit  $L, \frac{N_{\max}}{L} \rightarrow \infty$ .

### 3 Results

We have calculated the matrix elements of  $H$  restricted to  $V_{K_{\max}, D_{\max}}$  using a symbolic differentiation-integration algorithm<sup>4</sup> and diagonalized  $H$ , obtaining both eigenvalues and eigenstates. Let  $\Delta$  be the full propagator,

$$\Delta(p^2) = i \int d^2x e^{ip_\nu x^\nu} \langle 0 | T [\phi(x^\mu) \phi(0)] | 0 \rangle. \quad (11)$$

---

<sup>3</sup>In the case of spontaneous symmetry breaking, the broken symmetry of the vacuum may require retaining a large number of  $q_0$  modes. This however is remedied by shifting the variable,  $q'_0 = q_0 - \langle 0 | q_0 | 0 \rangle$ .

<sup>4</sup>All codes can be obtained by request from the authors.

We have computed  $\Delta$  by inserting our complete set of eigenstates (complete in  $V_{K_{\max}, D_{\max}}$ ). Let  $\Delta_{\text{mp}}$  be the multi-particle contribution to  $\Delta$ ,

$$\Delta_{\text{mp}}(p^2) = \Delta(p^2) - \Delta_{\text{pole}}(p^2), \quad (12)$$

where  $\Delta_{\text{pole}}$  is the single-particle pole contribution. We are primarily interested in  $\Delta_{\text{mp}}$ , a quantity that cannot be obtained for  $p^2 > 0$  using Monte Carlo methods. Since the imaginary part of  $\Delta_{\text{pole}}$  is a delta function, it is easy to distinguish the single-particle and multi-particle contributions in a plot of the imaginary part of  $\Delta$ . The real part of  $\Delta$ , however, is dominated by the one-particle pole. For this reason we have chosen to plot the real part of  $\Delta_{\text{mp}}$  rather than that of  $\Delta$ .

Although we have referred to multi-particle states, it should be noted that in our finite periodic box there are no true continuum multi-particle states. Instead we find densely packed discrete spectra with level separation of size  $\sim L^{-1}$  which become continuum states in the limit  $L \rightarrow \infty$ . We can approximate the contribution of these  $L \rightarrow \infty$  continuum states by a simple smoothing process. We included a small width  $\Gamma \sim L^{-1}$  to each of the would-be continuum states and averaged over a range of values for  $L$ . For the results we report here we have averaged over values  $L = 2.0\pi, 2.1\pi, \dots, 2.8\pi$ . For convenience all units have been scaled such that  $\mu = 1$ .

The parameter  $\zeta$  was adjusted to reduce the errors due to the finite cutoff values  $K_{\max}$  and  $D_{\max}$ . Since the spectrum of  $H$  is bounded below, errors due to finite  $K_{\max}$  and  $D_{\max}$  generally drive the estimated eigenvalues higher. One strategy, therefore, is to optimize  $\zeta$  by minimizing the trace of  $H$  restricted to the subspace  $V_{K_{\max}, D_{\max}}$ . The approach used here is a slight variation of this — we have minimized the trace of  $H$  restricted to a smaller subspace  $V_{K'_{\max}, D'_{\max}} \subset V_{K_{\max}, D_{\max}}$ . The aim is to accelerate the convergence of the lowest energy states rather than the entire space  $V_{K_{\max}, D_{\max}}$ . Throughout our analysis we used  $K'_{\max}, D'_{\max} = 8, 3$ .

For  $\frac{\lambda}{4t} = 0.50$  we have plotted the imaginary part of  $\Delta$  in Figure 1 and the real part of  $\Delta_{\text{mp}}$  in Figure 2. The value  $\frac{\lambda}{4t} = 0.50$  is above the threshold for reliable perturbative approximation<sup>5</sup> ( $\frac{\lambda}{4t} \lesssim 0.25$ ) but below the critical value at which  $\phi \rightarrow -\phi$  symmetry breaks spontaneously ( $\frac{\lambda}{4t} \approx 2.5$ ). The contribution of the one-particle state appears near  $p^2 = (0.93)^2$  and the three-particle threshold is at approximately  $p^2 = (2.9)^2$ . We have chosen several different values for  $N_{\max}, K_{\max}, D_{\max}$  to show the convergence as these parameters become large. The plot for  $N_{\max}, K_{\max}, D_{\max} = 9, 19, 7$  appears relatively close to the asymptotic limit. The somewhat bumpy texture of the curves is due to the finite size of our periodic box and diminishes with increasing  $L$ . From dimensional power counting, we expect errors for finite  $N_{\max}$  to scale as  $N_{\max}^{-2}$ . Assuming that  $K_{\max}$  and  $D_{\max}$  also function as uniform energy cutoffs, we expect a similar error dependence — and it appears plausible from the results in Figures 1 and 2. A more systematic analysis of the errors and extrapolation methods for finite  $N_{\max}, K_{\max}, D_{\max}$ , and  $L$ , will be discussed in future work.

<sup>5</sup>For momenta  $|p^2| \gtrsim 1$ .

In Figures 3 and 4 we have compared our spectral calculations with the two-loop perturbative result for  $\frac{\lambda}{4!} = 0.01$ . We have used  $N_{\max}, K_{\max}, D_{\max} = 9, 19, 7$ , and the agreement appears good. For small  $\frac{\lambda}{4!}$  the propagator has a very prominent logarithmic cusp at the three-particle threshold, which can be seen clearly in Figures 3 and 4.

In Figures 5 and 6 we have compared results for  $\frac{\lambda}{4!} = 0.25, 0.50, 1.00$ . We have again used  $N_{\max}, K_{\max}, D_{\max} = 9, 19, 7$ . In contrast with the quadratic scaling in the perturbative regime, the results here scale approximately linearly with  $\frac{\lambda}{4!}$ . An interesting and perhaps related observation is that the magnitude of the multi-particle contribution to  $\Delta$  remains small ( $\lesssim 0.003$ ) even for the rather large coupling value  $\frac{\lambda}{4!} = 1.00$ .

## 4 Limitations and new ideas

We now address the computational limits of the diagonalization techniques presented in this work. These techniques are rather straightforward and can in principle be generalized to any field theory. In practise however the Fock space  $V_{K_{\max}, D_{\max}}$  becomes prohibitively large, especially for higher dimensional theories. The data in Figures 1 and 2 and crosschecks with Euclidean Monte Carlo results<sup>6</sup> suggest that for  $N_{\max} = 9$  and  $L = 2.0\pi, \dots, 2.8\pi$  our spectral results with  $K_{\max}, D_{\max} = 19, 7$  and  $\frac{\lambda}{4!} < 1$  are within 20% of the  $K_{\max}, D_{\max} \rightarrow \infty$  limit. In this case  $V_{K_{\max}, D_{\max}}$  is a 2036 dimensional space and requires about 100 MB of RAM using general (dense) matrix methods.

Sparse matrix techniques such as the Lanczos or Arnoldi schemes allow us to push the dimension of the Fock space to about  $10^5$  states. This may be sufficient to do accurate calculations near the critical point  $\frac{\lambda}{4!} \approx 2.5$  for larger values of  $L$  and  $N_{\max}$ . It is, however, near the upper limit of what is possible using current computer technology and existing algorithms. Unfortunately field theories in  $2+1$  and  $3+1$  dimensions will require much larger Fock spaces, probably at least  $10^{12}$  and  $10^{18}$  states respectively. In order to tackle these larger Fock spaces it is necessary to venture beyond standard diagonalization approaches. The problem of large Fock spaces ( $\gg 10^6$  states) is beyond the intended scope of this analysis. But since it is of central importance to the diagonalization approach to field theory we would like to briefly comment on current work being done which may resolve many of the difficulties. The new approach takes advantage of the sparsity of the Fock-space Hamiltonian and the approximate (quasi-)sparsity of the eigenvectors. A detailed description will be provided in a future publication [9].

We start with some observations about the eigenvectors of the  $\phi_{1+1}^4$  Hamiltonian for  $N_{\max} = 9$ ,  $L = 2.5\pi$  and  $K_{\max}, D_{\max} = 19, 7$ . To make certain that we are probing non-perturbative physics we will set  $\frac{\lambda}{4!} = 2.5$ , the approximate critical point value. We label the normalized eigenvectors as  $|v_0\rangle, |v_1\rangle, \dots$ , ascending in order with respect to energy. We also define  $|b_0\rangle, |b_1\rangle, \dots$  as the

<sup>6</sup>See [3] for a discussion of these methods.

normalized eigenvectors of the free, non-interacting theory. For any  $v_i$  we know

$$\sum_j |\langle b_j | v_i \rangle|^2 = 1. \quad (13)$$

Let us define  $\| |v_i\rangle \|_{(n)}$  as the partial sum

$$\| |v_i\rangle \|_{(n)} = \sum_{k=1, \dots, n} |\langle b_{j_k} | v_i \rangle|^2, \quad (14)$$

where the inner products have been sorted from largest to smallest

$$|\langle b_{j_1} | v_i \rangle| \geq |\langle b_{j_2} | v_i \rangle| \geq \dots. \quad (15)$$

Table 1 shows  $\| |v_i\rangle \|_{(n)}$  for several eigenvectors and different values of  $n$ .

Table 1

$\   v_i\rangle \ _{(n)}$	$n = 10$	$n = 20$	$n = 40$	$n = 80$
$ v_0\rangle$	0.75	0.84	0.90	0.94
$ v_1\rangle$	0.89	0.92	0.95	0.97
$ v_5\rangle$	0.87	0.91	0.94	0.96
$ v_{10}\rangle$	0.77	0.86	0.90	0.94

Despite the non-perturbative coupling and complex phenomena associated with the phase transition, we see from the table that each of the eigenvectors can be approximated by just a small number of its largest Fock-space components. We recall that the Fock space for this system has 2036 dimensions. The eigenvectors are therefore quasi-sparse in this space, a consequence of the sparsity of the Hamiltonian. If we write the Hamiltonian as a matrix in the free Fock-space basis, a typical row or column contains only about 200 non-zero entries, a number we refer to as  $N_{\text{transition}}$ . In [9] we show that a typical eigenvector will be dominated by the largest  $\sqrt{N_{\text{transition}}}$  elements.<sup>7</sup> The key point is that  $\sqrt{N_{\text{transition}}}$  is quite manageable — on the order of  $10^3$  and  $10^5$  for  $2+1$  and  $3+1$  dimensional field theories respectively. Although the size of the Fock space for these systems are enormous, the extreme sparsity of the Hamiltonian suggests that the eigenvectors can be approximated using current computational resources.

With this simplification, the task is to find the important basis states for a given eigenvector. Since the important basis states for one eigenvector are generally different from that of another, each eigenvector is determined independently. This provides a starting point for parallelization, and many eigenvectors can be determined at the same time using massively parallel computers. In [9] we present a simple stochastic algorithm where the exact eigenvectors act as stable fixed points of the update process.

<sup>7</sup>There are some special exceptions to this rule and they are discussed in [9]. But these are typically not relevant for the lower energy eigenstates of a quantum field Hamiltonian.

## 5 Summary

We have introduced a spectral approach to periodic field theory and used it to calculate the propagator in  $1 + 1$  dimensional  $\phi^4$  theory. We find that the straightforward application of these methods with existing computer technology can be useful for describing the multi-particle properties of the theory, information difficult to obtain using Euclidean Monte Carlo methods. However the extension to higher dimensional theories is made difficult by the large size of the corresponding Fock space. As a possible solution to this problem, we note that each eigenvector of the  $\phi_{1+1}^4$  Hamiltonian can be well-approximated using relatively few components and discuss some current work on quasi-sparse eigenvector methods.

## Acknowledgment

We thank Eugene Golowich, Mark Windoloski, and Daniel Lee for useful discussions. D.L. also thanks the organizers and participants of the CSSM Workshop on Light-Cone QCD and Non-perturbative Hadron Physics in Adelaide. We acknowledge financial support provided by the NSF under Grant 5-22968 and PHY-9802709.



## References

- [1] D. Lee, Phys. Lett. B439 (1998) 85; D. Lee, Phys. Lett. B444 (1998) 474; B. Borasoy, D. Lee, Phys. Lett. B447 (1999) 98; D. Lee, N. Salwen, Phys. Lett. B460 (1999) 107.
- [2] N. Salwen, D. Lee, Phys. Lett. B468 (1999) 118.
- [3] P. Marrero, E. Roura, D. Lee, Phys. Lett. 471(1999) 45.
- [4] E. Brooks III, S. Frautschi, Z. Phys. C23 (1984) 263; E. Brooks III, S. Frautschi, Z. Phys. C14 (1982) 27.
- [5] L. Hollenberg, Phys. Rev. D47 (1993) 1640; L. Hollenberg, Phys. Rev. D50 (1994) 2293.
- [6] R. Perry, A. Harindranath, K. Wilson, Phys. Rev. Lett. 24 (1990) 2959.
- [7] S. Pinsky, B. van de Sande, J. Hiller, Phys. Rev. D51 (1995) 726; C. Bender, S. Pinsky, B. van de Sande, Phys. Rev. D48 (1993) 816.
- [8] S. Brodsky, H. Pauli, S. Pinsky, Phys. Rep. 301 (1998) 299.
- [9] De. Lee, N. Salwen, Da. Lee, work in progress.

## Figures

Figure 1: Imaginary part of  $\Delta(p^2)$  for  $\frac{\lambda}{4!} = 0.50$  and several values for  $N_{\max}, K_{\max}, D_{\max}$ .

Figure 2: Real part of  $\Delta_{\text{mp}}(p^2)$  for  $\frac{\lambda}{4!} = 0.50$  and several values for  $N_{\max}, K_{\max}, D_{\max}$ .

Figure 3: Imaginary part of  $\Delta(p^2)$  for  $\frac{\lambda}{4!} = 0.01$  and comparison with the two-loop result.

Figure 4: Real part of  $\Delta_{\text{mp}}(p^2)$  for  $\frac{\lambda}{4!} = 0.01$  and comparison with the two-loop result.

Figure 5: Imaginary part of  $\Delta(p^2)$  for  $\frac{\lambda}{4!} = 0.25, 0.50, 1.00$ .

Figure 6: Real part of  $\Delta_{\text{mp}}(p^2)$  for  $\frac{\lambda}{4!} = 0.25, 0.50, 1.00$ .

Figure 1

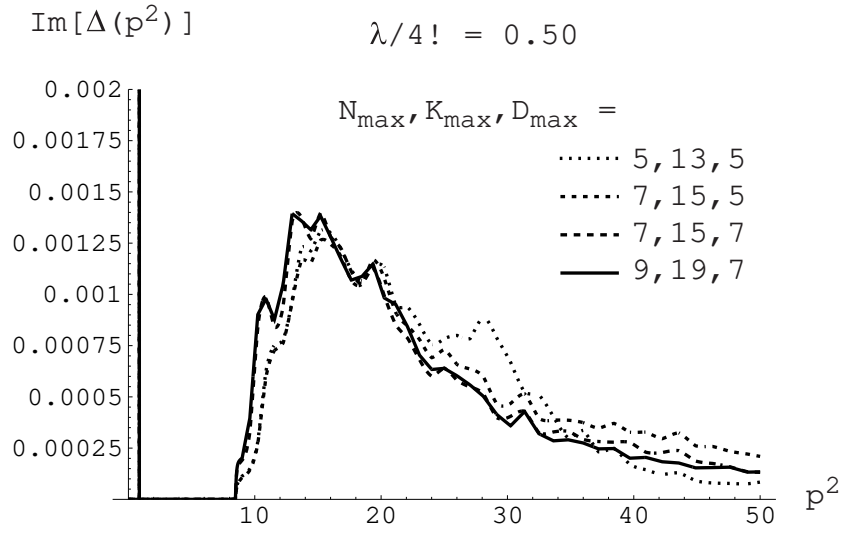


Figure 2

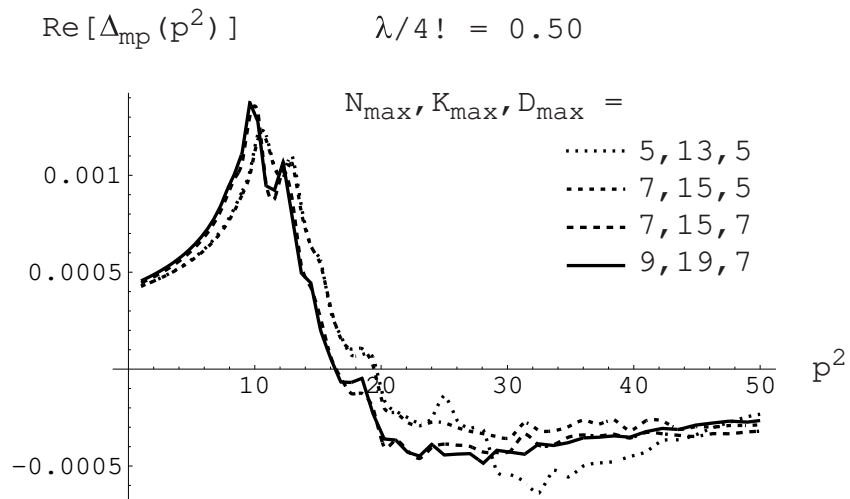


Figure 3

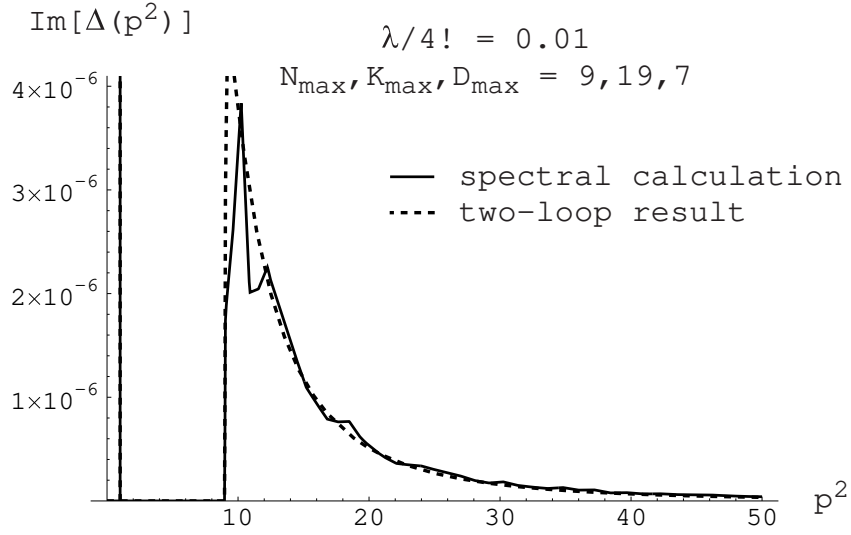


Figure 4

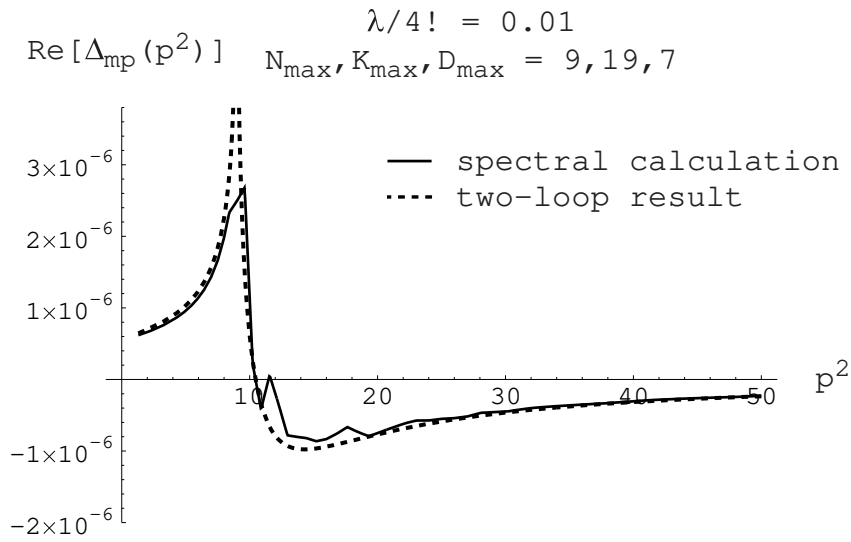


Figure 5

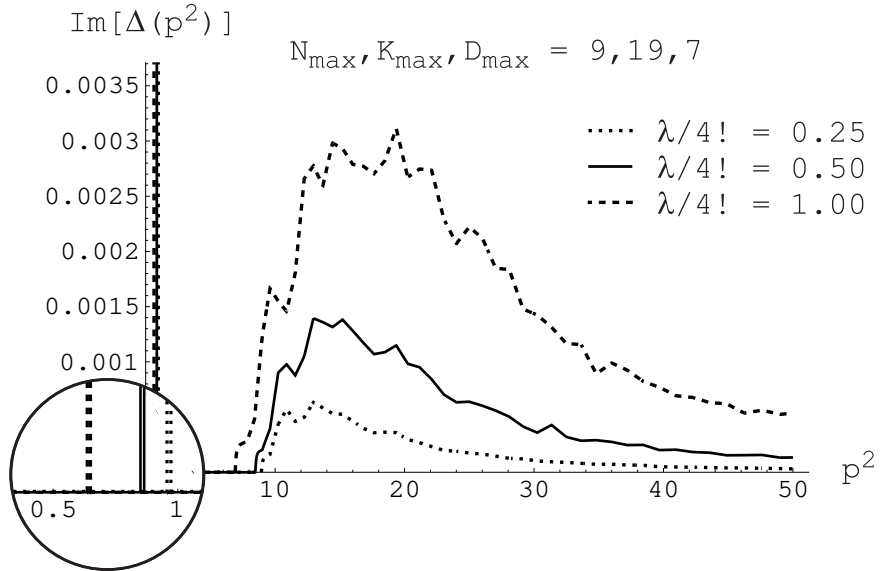


Figure 6

